# Carbon Monoxide Oxidation over Chromium Sesquioxide. III. Kinetics of the Reaction

Masayoshi KOBAYASHI and Haruo KOBAYASHI

*Department of Chemical Process Engineering, Faculty of Engineering, Hokkaido University, Sapporo 060*

(Received August 4, 1975)

Based on the experimental findings in Parts I and II, mechanisms of carbon monoxide oxidation over $\alpha$-$Cr_2O_3$ were proposed with which the reaction takes place simultaneously through two parallel reaction paths. Overall reaction consists of five elementary steps, and the rate constants of all ellementary stepes were determined from the analysis of appropriate transient response data. The simulation of transient response with these rate constants proved the validity of these mechansims and the results of kinetic analyses.

The reaction mechanism of carbon monoxide oxidation over $Cr_2O_3$ has been studied by several investigators and the conclusions reached by these investigators are rather divergent. Winter[1] thought that the rate determining step was the adsorption of oxgen. Tarama, Teranishi, and Hattori[2] worked out the kinetic analysis of the data obtained in a closed recycle reaction system and suggested that the overall reaction was controlled by the reaction between adsorbed carbon monoxide and adsorbed atomic oxygen. Recently, Davydov, Shchekochikhin, and Keier[3] suggested, on the basis of IR spectroscopic study of surface complexes formed on $\alpha$-$Cr_2O_3$, that the rate determing step was not the adsorption of oxygen but either the reaction of gaseous carbon monoxide with surface oxygen species or the desorption of surface complexes formed in the course of the reaction.

Voltz and Weller[4] pointed out in early days that the catalytic activity of $Cr_2O_3$ was affected by the oxidation states of the surface. Recently, the complexity of the characteristics of $Cr_2O_3$ surface has been revealed in detail by IR spectroscopic studies.[5-9] The divergent conclusions drawn by many investigators for the kinetics of CO oxidation over $Cr_2O_3$, therefore, may be attributable to the different characteristics of samples, which is highly sensitive to pretreatments, temperature, and ambient gas atmosphere.

In our previous paper, Part I,[10] it was concluded that oxygen is adsorbed dissociatively on coordinatively unsaturated chromium ions forming oxygen anions, and that the oxygen anions consist of two groups, $O^-\cdot S_I$ and $O^-\cdot S_{II}$, the former is very rapidly generated and easily reacts with CO while the latter is produced very slowly and is less active for the reaction with CO. It was also shown[11] that CO could not be adsorbed on $\alpha$-$Cr_2O_3$ surface when it was either fully oxidized or in steady states where CO oxidation was taking place. These results lead to a conclusion that the oxidation of CO over $\alpha$-$Cr_2O_3$ proceeds through the reaction between gaseous CO and oxygen anions on the surface.

In the present paper, we are concerned with how the different groups of the oxygen anions take part in the oxidation of CO, and also with the detailed kinetic analysis of the reaction.

## Reaction Mechanism for Kinetic Analysis

According to the results and the discussion in the previous paper, the mechanism of the oxidation of CO over $Cr_2O_3$ catalyst can be summarized as follows.

a) Two kinds of dissociatively adsorbed oxygen anions, $O^-\cdot S_I$ and $O^-\cdot S_{II}$, are present on the surface and both are active for the oxidation of CO. $O^-\cdot S_I$ has a higher oxidation power and can be rapidly regenerated by gaseous oxygen. Therefore, $S_I$ is always saturated with adsorbed oxygen anions under the steady states of the reaction at various partial pressure of CO. On the other hand, $O^-\cdot S_{II}$ has a lower oxidation power and the rate of its regeneration is slow and hence the concentration of $O^-\cdot S_{II}$ decreased with higher partial pressure of CO with which the reaction rates are higher.

b) Under the steady states of the reaction, the reaction proceeds through the simultaneous reactions of gaseous CO with both $O^-\cdot S_I$ and $O^-\cdot S_{II}$ with different reaction rates.

c) Carbon dioxide produced by the reaction between CO and $O^-\cdot S_I$ is adsorbed irreversibly on $S_I$ when oxygen is not present in the gas phase, but when oxygen exists in the gas phase the adsorbed $CO_2$ on $S_I$ is very rapidly desorbed due to the competitive adsorption of oxygen onto $S_I$. On the other hand, the desorption of carbon dioxide produced by the reaction between CO and $O^-\cdot S_{II}$ is not affected by the presence of oxygen in the gas phase. Under the steady states of the reaction, the amount of adsorbed $CO_2$ on $S_{II}$ is negligibly small.

d) The adsorbed $CO_2$ on $S_I$ and $S_{II}$ is not ionized.

The reaction mechanism suggested above for the catalytic oxidation of CO over $Cr_2O_3$ can be represented in the sequence of the following steps.

Reaction path I:

$$CO(g) + O^-\cdot S_I \xrightarrow{k_1} CO_2\cdot S_I + e \quad (1)$$

$$O_2(g) + 2CO_2\cdot S_I + 2e \xrightarrow{k_2} 2CO_2(g) + 2O^-\cdot S_I \quad (2)$$

Reaction path II:

$$CO(g) + O^-\cdot S_{II} \xrightarrow{k_3} CO_2\cdot S_{II} + e \quad (3)$$

$$CO_2\cdot S_{II} \xrightarrow{k_4} CO_2(g) + S_{II} \quad (4)$$

$$O_2(g) + 2S_{II} + 2e \xrightarrow{k_5} 2O^-\cdot S_{II} \quad (5)$$

Although non-ionized adsorption of $CO_2$ was suggested in the previous paper[11], one can see another evidence in the results shown in Fig. 1, which indicate that the shift of electrons takes place when gaseous CO reacts with the surface oxygen anions.

Let us examine the results shown in Fig. 1. After the catalyst had been completely oxidized by a stream

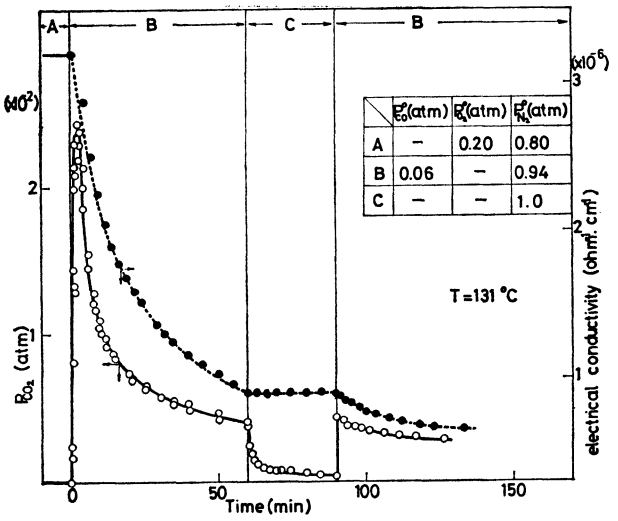


Fig. 1. $CO$-$CO_2$ and $CO$-$\sigma$ response.

of $O_2$(20%)-$N_2$ mixture, the stream was suddenly replaced by a stream of CO(6%)-$N_2$ mixture and the responses in the outlet $CO_2$ concentration and in the electrical conductivity of the catalyst were followed for 60 min. The $CO_2$ concentration reached a maximum in a very short time and then fell down steeply and afterwards it gradually decreased to very low values. The electrical conductivity, on the other hand, decreased monotonously due to the formation of gaseous $CO_2$ with the expense of oxygen anions on the surface. Since the catalyst is a p-type semiconductor, the picking up of surface oxygen by CO in the form of $CO_2$ results in the decrease in the conductivity, due to the shift of electrons from the oxygen anions back to the catalyst. After 60 min, the feed was replaced by a stream of pure nitrogen. Even with no carbon monoxide in the feed, $CO_2$ could be detected for a certain period of time due to the desorption of $CO_2$ which had been produced and accumulated on the surface during the foregoing reduction period. The electrical conductivity, on the other hand, was kept entirely constant during this run. These results substantiate the Steps (1) and (2) which indicate that the electron transfer back to the catalyst occurs when the surface compounds are formed by the reaction of CO with surface oxygen anions, and not when the surface compound decomposes to give gaseous $CO_2$ as has been suggested by Matsushita, Nakata[12] and Courtois and Teichner.[13]

## Determination of Rate Constants

The rate constants $k_2$ and $k_5$ have been already determined in Part I[10] as $k_I$ and $k_{II}$, respectively.

$$k_2 = k_I = 1.75\times10^{-4}\ \text{mol/g min atm}$$

$$k_5 = k_{II} = 4.8\times10^{-6}\ \text{mol/g min atm}$$

*Determination of* $k_4$. The value of $k_4$ can be determined from the CO(dec., 0)-$CO_2$ response during the reaction under steady states. An example of the CO-(dec., 0)-$CO_2$ response data is shown in Fig. 2. As has been discussed in Part II,[11] the desorption of $CO_2$ produced by gaseous CO and $O^-\cdot S_I$ on the surface

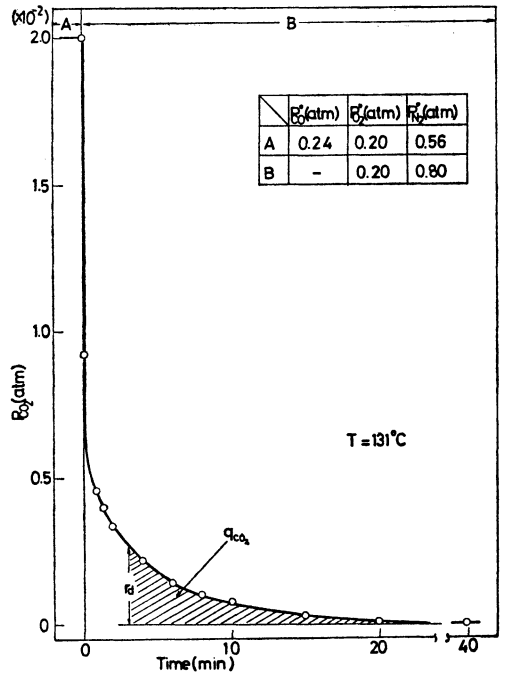


Fig. 2. CO(dec., 0)-$CO_2$ response during the reaction.

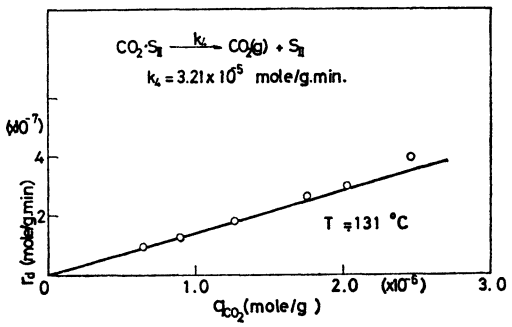


Fig. 3. Plot of the desorption rate of $CO_2$ *vs.* $q_{CO_2}$ estimated from the graphical analyses of the curve presented in Fig. 2.

is very rapid due to the competitive adsorption of oxygen, then the slow desorption of $CO_2$ as can be seen in the later part of the response may be attributed solely to the desorption of $CO_2$ from $CO_2\cdot S_{II}$. Furthermore, it is known that the amount of $CO_2$ readsorbed from gas phase on $S_{II}$ during the reaction is negligible.[11] Therefore, the rates of $CO_2$ desorption measured in the later part of the response can be considered to give true rates of $CO_2$ desorption from $CO_2\cdot S_{II}$. From the response data, one can estimate the amounts of adsorbed $CO_2\cdot S_{II}$ and the corresponding desorption rates of $CO_2$. A plot of desorption rates against the adsorbed amounts of $CO_2$ gives a straight line as presented in Fig. 3. The rate of $CO_2$ desorption from $CO_2\cdot S_{II}$ can be given by

$$r_d = k_4\cdot\theta_{II}\cdot CO_2 \qquad (6)$$

where $k_4$ is the desorption rate constant of $CO_2$ from $S_{II}$ and $\theta_{II\cdot CO_2}$ is the fractional coverage of $S_{II}$ with $CO_2$. Assuming linear form of adsorbed $CO_2$ on $S_{II}$, as has been discussed in Part II,[11] the saturated amount of $CO_2\cdot S_{II}$, $q_{CO_2\cdot max}$, may be taken as equivalent to that of $O^-\cdot S_{II}$ as estimated in Part I, which is equal

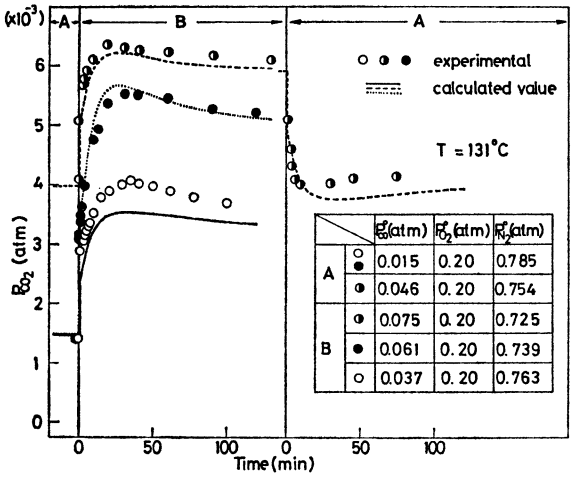


| | | $P^0_{CO}$(atm) | $P^0_{O_2}$(atm) | $P^0_{N_2}$(atm) |
|---|---|---|---|---|
| A | ○ | 0.015 | 0.20 | 0.785 |
| | ◑ | 0.046 | 0.20 | 0.754 |
| B | ◑ | 0.075 | 0.20 | 0.725 |
| | ● | 0.061 | 0.20 | 0.739 |
| | ○ | 0.037 | 0.20 | 0.763 |

Fig. 4. CO-$CO_2$ response.

to $2.34\times10^{-4}$ mol/g. Using this value and the slope of the straight line in Fig. 3, one can estimate the value of $k_4$ as

$$k_4 = 3.21\times10^{-5} \text{ mol/g min}$$

Under the conditions given in Fig. 2, $\theta_{II\cdot CO_2}$ for the catalyst having been operated in the gas mixture A under the steady state was also estimated as

$$\theta_{II\cdot CO_2} = 0.017$$

*Determination of* $k_1$. $k_1$ can be determined from the CO–$CO_2$ response during the reaction at steady states. An example of such response is given in Fig. 4, which shows an instantaneous increase in $P_{CO_2}$ followed by a gradual increase to a maximum and then approaches a new steady state. The initial instantaneous increase in $P_{CO_2}$ may be ascribed to the rapid desorption of incremental $CO_2$ produced by the reaction of $O^-\cdot S_I$ and the increment of the partial pressure of CO. Because, as has been discussed in Part II, the $CO_2$ produced on $S_I$ can be desorbed very rapidly by the competitive adsorption of oxygen while that produced on $S_{II}$ desorbs gradually as we have seen in the foregoing sections. A plot of $\Delta r_1$ *vs.* $\Delta P_{CO}$ gives a linear relationship as presented in Fig. 5. Thus the initial increase in the production rate of $CO_2$, namely the rate of Step (1), can be given as

$$\Delta r_1 = k_1\cdot\theta_I\cdot\Delta P_{CO} \tag{8}$$

where $\theta_I$ is the fractional coverage of $S_I$ with oxygen. Since it is known that $\theta_I$ can be taken to be unity, the valu of $k_1$ can be estimated from the slope of the straight line in Fig. 5 as

$$k_1 = 4.15\times10^{-6} \text{ mol/g min atm.}$$

*Determination of* $k_3$. At the reaction steady state, the rate of $CO_2$ formation canbe expressed by the sum of both Eqs. 1 and 3 as follows:

$$r_{st} = k_1P_{CO}\theta_I + k_3P_{CO}\theta_{II} = r_I + r_{II} \tag{7}$$

where $r_I=k_1P_{CO}\theta_I$ and $r_{II}=k_3P_{CO}\theta_{II}$. Using the values of $k_1$ and $\theta_I$ estimated in the foregoing section, one can calculate $r_I$ and determine $r_{st}$ from the experimental data at various partial pressures of

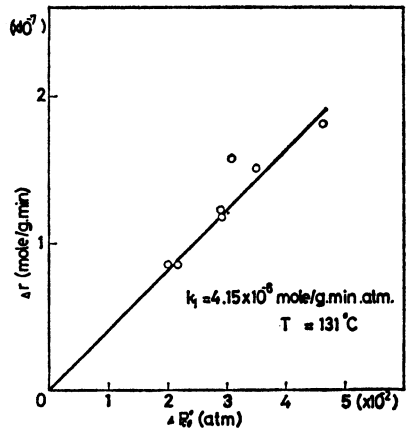


Fig. 5. Plot of $\Delta r$ *vs.* $\Delta P^0_{CO}$.

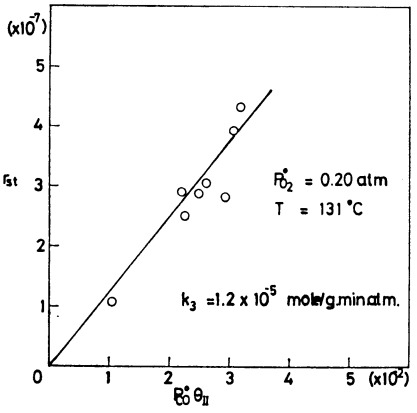


Fig. 6. Plot of $r_{st}$ *vs.* $P^0_{CO}\theta_{II}$.

CO. Therefore, $r_{II}$ at various partial pressures of CO is estimated easily from the difference between $r_{st}$ and $r_I$ at corresponding conditions.

On the other hand, the values of $\theta_{II}$ at the corresponding steady states can be roughly estimated from the electrical conductivity at the same conditions, which shows the amount of $O^-\cdot S_{II}$ since $S_I$ is fully occupied by oxygen anions due to its rapid adsorption during the reaction. A plot of $r_{II}$ against $\theta_{II}$ gives a straight line as shown in Fig. 6. From the slope of the straight line, the value of $k_3$ can be estimated as

$$k_3 = 1.2\times10^{-5} \text{ mol/g min atm.}$$

## Simulation of Response Data

From the analyses presented in the foregoing section, it is seen that $k_2$ is very much larger than $k_1$, *i.e.* the Step (1) is the rate determining step of the reaction path I. Hence the rate of $CO_2$ formation through reaction path I can be expressed by the following equation.

$$\frac{dP_{CO_2}}{dt} = k_2\theta_IP_{CO} \tag{9}$$

Based on this simplification, the unsteady-state mass balance equations for each component for over-all reaction can be given by[14]

$$\frac{dP_{CO}}{dt} = \frac{2U}{\varepsilon L}(P^0_{CO}-P_{CO}) - \frac{2\rho_cRT}{\varepsilon}(k_1P_{CO}\theta_I+k_3P_{CO}\theta_{II}) \tag{10}$$

$$\frac{dP_{CO_2}}{dt}=\frac{2U}{\varepsilon L}(P^0_{CO_2}-P_{CO_2})+\frac{2\rho_c RT}{\varepsilon}\times(k_1P_{CO}\theta_I+k_4\theta_{II\cdot CO_2}) \quad (11)$$

$$\frac{dP_{O_2}}{dt}=\frac{2U}{\varepsilon L}(P^0_{O_2}-P_{O_2})-\frac{2\rho_c RT}{\varepsilon}\times\left(\frac{1}{2}k_1P_{CO}\theta_I+k_5P_{O_2}\theta^2_{II\cdot v}\right) \quad (12)$$

$$\frac{d\theta_{II}}{dt}=\frac{1}{q_{O_2}}(2k_5P_{O_2}\theta^2_{II\cdot v}-k_3P_{CO}\theta_{II}) \quad (13)$$

$$\frac{d\theta_{II\cdot CO_2}}{dt}=\frac{1}{q_{CO_2}}(k_3P_{CO}\theta_{II}-k_4\theta_{II\cdot CO_2}) \quad (14)$$

where $\varepsilon$ abd $\rho_c$ are, respectively, void fraction and apparent density of the catalyst bed, and $U$ is the superficial velocity of the feed, $L$ the length of the catalyst bed. $\theta_{II\cdot v}$ is the fraction of vacant site $S_{II}$ and this is given by

$$\theta_{II\cdot v}=1-(\theta_{II}+\theta_{II\cdot CO_2}) \quad (15)$$

Suppose the reaction system is in the steady state with a feed containing CO and $O_2$ as the reactants, and the partial pressure of CO in the feed is suddenly increased from $P^{io}_{CO}$ to $P^{no}_{CO}$, then the inital conditions for the transient response will be given by these equations

$$\left.\begin{array}{ll}P^0_{CO}=P^{n0}_{CO} & \\ P^0_{CO_2}=0 & \text{inflow}\\ P^0_{O_2}=P^{i0}_{O_2} & \end{array}\right\}$$
$$\left.\begin{array}{ll}P_{CO}=P^{is}_{CO} & \\ P_{CO_2}=P^{is}_{CO_2} & \text{outflow}\\ P_{O_2}=P^{is}_{O_2} & \end{array}\right\}$$
$$\left.\begin{array}{ll}\theta_{II}=\theta^{is}_{II} & \\ \theta_{II\cdot CO_2}=\theta^{is}_{II\cdot CO_2} & \text{on the surface}\end{array}\right\} \text{ at } t=0 \quad (16)$$

In order to examine the validity of the $k_j$ values estimated so far, let us simulate the CO–$CO_2$ response data given in Fig.4. Although $P^{is}_{CO}$, $P^{is}_{CO_2}$, and $P^{is}_{O_2}$ can be obtained experimentally, these values are also calculated from initial inflow conditions given in Fig. 4 with $k_j$ values using Eqs. 10—14 under steady state conditions. For this calculation $\theta^{is}_{II}$ and $\theta^{is}_{II\cdot CO_2}$ are not known experimentally but can be calculated as follows as a function of $P^{is}_{CO}$ and $P^{is}_{O_2}$.

Under the initial steady state,

$$\frac{d\theta_{II}}{dt}=0 \quad (17)$$

Then from Eq. 13,

$$2k_5P^{is}_{O_2}(1-\theta^{is}_{II}-\theta^{is}_{II\cdot CO_2})^2-k_3P^{is}_{CO}\theta^{is}_{II}=0 \quad (18)$$

Since $\theta_{II\cdot CO_2}$ is very small as has been stated in a previous section, Eq. 18 can be simplified as

$$(\theta^{is}_{II})^2-(2+a)\theta^{is}_{II}+1=0 \quad (19)$$

where

$$a=k_3P^{is}_{CO}/2k_5P^{is}_{O_2} \quad (20)$$

Solving Eq. 19, one can obtain

$$\theta^{is}_{II}=\frac{1}{2}(2+a-\sqrt{a^2+4a}) \quad (21)$$

In the same way, $\theta^{is}_{II\cdot CO_2}$ can be obtained from Eq. 21 and Eq. 14 under steady states.

$$\theta^{is}_{II\cdot CO_2}=\frac{k_3}{2k_4}P_{CO}(2+a-\sqrt{a^2+4a}) \quad (22)$$

By these calculations the initial conditions, Eq. 16, for the response can be obtained. With these initial conditions, Eqs. 10—14 can be solved numerically. The time courses of the $P_{CO_2}$ change thus calculated for four different cases are shown in Fig. 4. The characteristic nature of the response data is simulated fairly well and this would indicate the validity of the proposed mechanisms and the values of $k_j$ estimated so far.

## Discussion

Here we shall summerize the values of $k_j$.

$k_1 = 4.15\times10^{-6}$ mol/g min atm

$k_2\ (=k_{II}) = 1.75\times10^{-4}$ mol/g min atm

$k_3 = 1.2\times10^{-5}$ mol/g min atm

$k_4 = 3.21\times10^{-5}$ mol/g min

$k_5\ (=k_{II}) = 4.8\times10^{-6}$ mol/g min atm

It is seen that $k_2$ is much larger than $k_1$ and this fact is quite consistent with the conclusion reached experimentally in Part II that the regeneration of $O^-\cdot S_I$ is very rapid and $O^-\cdot S_I$ always contributes to the reaction. It is seen also that $k_5$ is much smaller than $k_3$ and $k_4$. These results are also consistent with the conclusion drawn from the experimental findings in Parts I and II that the regeneration of $O^-\cdot S_{II}$ is slow and the concentration of $O^-\cdot S_{II}$ during the reaction under steady states is lowered when the reaction is opperated under higher partial pressures of CO, where the rates of picking up of $O^-\cdot S_{II}$ are higher.

Since $k_1$ and $k_3$ include the total number of $O^-\cdot S_I$ and $O^-\cdot S_{II}$, respectively, the true activity of each oxygen should be compared by the activity of single oxygen. Total amount of $O^-\cdot S_I$ is $3.3\times10^{-5}$ mol/g and that of $O^-\cdot S_{II}$ is $1.17\times10^{-4}$ mol/g and hence the true activity of each oxygen would be

$$k_1' = k_1/3.3\times10^{-5} = 1.26\times10^{-1}\ \text{min}^{-1}\,\text{atm}^{-1}$$

$$k_3' = k_3/1.17\times10^{-4} = 1.02\times10^{-1}\ \text{min}^{-1}\,\text{atm}^{-1}$$

$k_1'$ is only slightly larger than $k_3'$ and it seems to be not exactly consistent with the experimental findings in Part I, which suggest the higher reactivity of $O^-\cdot S_I$ compared to that of $O^-\cdot S_{II}$. The reason for this inconsistency may be ascribed to the difference in the activation energy of both types of oxygen species because the temperatures of reaction were different in both experiments. At the present moment, however, this problem is still open to the question and will need further investigations.

## Nomenclature

$a$: defined in Eq. 20.

$k_j$: rate coefficient for step $j$, arbitrary unit.

$L$: total length of the catalyst bed (cm).

$P_{O_2}$, $P_{CO}$, $P_{CO_2}$: partial pressure of oxygen, carbon monoxide, and carbon dioxide at the outlet of the catalyst bed at the un-

steady state, respectively (atm).

$P^0_{O_2}$, $P^0_{CO}$, $P^0_{CO_2}$: partial pressure of oxygen, carbon monoxide, and carbon dioxide at the inlet of the catalyst bed, respectively (atm).

$P^{i0}_{O_2}$, $P^{i0}_{CO}$: partial pressure of oxygen and carbon monoxide at the inlet of the catalyst bedat initial steady state, respectively (atm).

$P^{n0}_{CO}$: newly set partial pressure of carbon monoxide at the inlet of the catalyst bed (atm).

$P^{is}_{O_2}$, $P^{is}_{CO}$, $P^{is}_{CO_2}$: partial pressure of oxygen, carbon monoxide, and carbon dioxide at the outlet of the catalyst bed at initial steady state, respectively (atm).

$q_{CO_2}$, $q_{CO_2}$: total amounts of $O_2$ and $CO_2$ adsorbed on active site $S_{II}$, respectively (mol/g).

$R$: gas constant, consistent units.

$S_I$, $S_{II}$: active sites on the surface denoted in earlier paper.[10]

$t$: time elapsed after the step change of gas composition (min).

$T$: temperature (K).

$U$: superficial gas velocity (cm/min).

*Greek Symbols*

$\varepsilon$: void fraction of packed bed of reactor (—).

$\theta_{II}$, $\theta_{II\cdot CO_2}$: coverage averaged in the catalyst bed for $O^-\cdot S_{II}$ and $CO_2\cdot S_{II}$, respectively (—).

$\theta^{is}_{II}$, $\theta^{is}_{II\cdot CO_2}$: coverage averaged in the catalyst bed for $O^-\cdot S_{II}$ and $CO_2\cdot S_{II}$ at the steady state of reaction, respectively (—).

$\theta_{II\cdot v}$: fraction of vacant active sites $S_{II}$ (—).

$\rho_c$: catalyst bed density (g/cm$^3$).

**Refereences**


1) E. R. S. Winter, *J. Chem. Soc.*, **1955**, 2726.

2) K. Tarama, S. Teranishi, and K. Hattori, *Kogyo Kagaku Zasshi*, **63**, 714 (1960).

3) A. A. Davydov, M. Yu. Shchekochikhin, and P. N. Keier, *Kinet. Katal.*, **10**, 1341 (1969).

4) S. E. Voltz and S. W. Weller, *J. Phys. Chem.*, **59**, 566 (1955).

5) M. Yu. Shchekochikhin, G. I. Panov, and N. A. Akulich, *Kinet. Katal.*, **9**, 1315 (1968).

6) A. A. Davydov, M. Yu. Schekochikhin, P. N. Keier, and A.P. Zeif, *Kinet. Katal.*, **10**, 1125 (1969).

7) A. Zecchina, S. Coluccia, E. Guglielminotti, and G. Ghiotti, *J. Phys. Chem.*, **76**, 2774 (1971).

8) A. Zecchina, S. Coluccia, L. Cerruti, and E. Borello, *J. Phys. Chem.*, **76**, 2783 (1971).

9) A. Zecchina, S. Coluccia, E. Guglielminotti, and G. Ghiotti, *J. Phys. Chem.*, **76**, 2790 (1971).

10) M. Kobayashi and H. Kobayashi, *Bull. Chem. Soc. Jpn.*, **49**, 3009 (1976).

11) M. Kobayashi, T. Date, and H. Kobayashi, *Bull. Chem. Soc. Jpn.*, **49**, 3014 (1976).

12) S. Matsushita and T. Nakata, *J. Chem. Phys.*, **36**, 665 (1962).

13) M. Courtois and S. T. Teichner, *J. Catal.*, **1**, 121 (1962).

14) H. Kobayashi and M. Kobayashi, *Catal. Rev.*, **10**, 139 (1974).